Received: 13 November 2017 | Revised: 20 December 2017 | Accepted: 28 December 2017

DOI: 10.1002/hbm.23949

RESEARCH ARTICLE

WILEY

Default mode network modifications in Fabry disease: A resting-state fMRI study with structural correlations

Sirio Cocozza[1] | Giuseppe Pontillo[1] | Mario Quarantelli[2] | Francesco Saccà[3] | Eleonora Riccio[4] | Teresa Costabile[3] | Gaia Olivo[5] | Vincenzo Brescia Morra[3] | Antonio Pisani[4] | Arturo Brunetti[1] | Enrico Tedeschi[1] | on behalf of AFFINITY study group

[1]Department of Advanced Biomedical Sciences, University "Federico II,", Naples, Italy

[2]Institute of Biostructure and Bioimaging, National Research Council, Naples, Italy

[3]Department of Neurosciences and Reproductive and Odontostomatological Sciences, University "Federico II,", Naples, Italy

[4]Department of Public Health, Nephrology Unit, University "Federico II,", Naples, Italy

[5]Department of Neuroscience, Uppsala University, Uppsala, Sweden

Correspondence
Giuseppe Pontillo, Department of Advanced Biomedical Sciences, University "Federico II", Via Pansini, 5, 80131 Naples, Italy.
Email: giuseppe.pon@gmail.com

Abstract

Aim of the study was to evaluate the presence of Default Mode Network (DMN) modifications in Fabry Disease (FD), and their possible correlations with structural alterations and neuropsychological scores. Thirty-two FD patients with a genetically confirmed diagnosis of classical FD (12 males, mean age 43.3 ± 12.2) were enrolled, along with 35 healthy controls (HC) of comparable age and sex (14 males, mean age 42.1 ± 14.5). Resting-State fMRI data were analyzed using a seed-based approach, with six different seeds sampling the main hubs of the DMN. Structural modifications were assessed by means of Voxel-Based Morphometry (VBM) and Tract-Based Spatial Statistics analyses. Between-group differences and correlations with neuropsychological variables were probed voxelwise over the whole brain. Possible correlations between FC modifications and global measures of microstructural alteration were also tested in FD patients with a partial correlation analysis. In the FD group, clusters of increased functional connectivity involving both supratentorial and infratentorial regions emerged, partially correlated to the widespread white matter (WM) damage found in these patients. No gray matter volume differences were found at VBM between the two groups. The connectivity between right inferior frontal gyrus and precuneus was significantly correlated with the Corsi block-tapping test results ($p = .0001$). Widespread DMN changes are present in FD patients that correlate with WM alterations and cognitive performance. Our results confirm the current view of a cerebral involvement in FD patients not simply associated to major cerebrovascular events, but also related to significant and diffuse microstructural and functional changes.

KEYWORDS

fabry disease, default mode network, resting-state fMRI, tract-based spatial statistics

1 | INTRODUCTION

Fabry disease (FD) is a rare X-linked metabolic disorder caused by a deficiency in the lysosomal enzyme α-galactosidase A (Germain, 2010), which causes an accumulation of the incompletely catabolized substrate, globotriaosylceramide (Gb3), in a variety of cell types and organs throughout life. This accumulation leads to multiorgan pathology that most seriously affects the kidneys, heart, and the cerebrovascular system.

Cerebral involvement is common in FD, mainly caused by endothelial accumulation of Gb3 causing cerebrovascular complications (Kolodny et al., 2015). The resulting cerebral vasculopathy includes stroke, which is the most prevalent cerebrovascular event in FD (Sims, Politei, Banikazemi, & Lee, 2009), with a prevalence of up to 7.0% in Fabry patient registries, and white matter (WM) lesions, often clinically asymptomatic in these patients (Fellgiebel et al., 2006a).

Sirio Cocozza and Giuseppe Pontillo contributed equally to this study.

Neuropsychological symptoms are common in FD, in particular depression, reported to be clinically significant in up to 50% of the patients (Cole et al., 2007). Furthermore, existing data suggest an impairment in executive functioning, information processing speed and attention, although with a preservation of global cognitive functioning (Bolsover, Murphy, Cipolotti, Werring, & Lachmann, 2014).

Resting-state functional MRI (RS-fMRI) analysis allows to demonstrate the presence of preferential functional connectivity (FC) between specific cerebral structures, which are organized in stable and simultaneously operating networks. Among these networks, a central role is played by the so-called Default Mode Network (DMN) (Raichle, 2015), which is involved in the coordination of sensorimotor and cognitive goal-directed activities, and in functions related to "mind wandering," so that it has been proposed to play an adaptive role in internal mentation (Andrews-Hanna, 2012). Abnormalities of the DMN, detected by the analysis of RS-fMRI data, have been demonstrated in several disorders, such as Alzheimer's disease (Vemuri, Jones, & Jack, 2012), Parkinson's disease (Prodoehl, Burciu, & Vaillancourt, 2014), depression (Dutta, McKie, & Deakin, 2014), Huntington's disease (Quarantelli et al., 2013), schizophrenia (Argyelan et al., 2014), and epilepsy (Cataldi, Avoli, & de Villers-Sidani, 2013).

To the best of our knowledge, no studies have been performed to evaluate the integrity of the DMN in FD, a condition in which FC alterations of the motor cortex have been recently reported (Cocozza et al., 2017). Therefore, we aimed to assess in these patients the DMN status, simultaneously investigating the possible association of macrostructural modifications in the gray matter (GM) by means of Voxel-Based Morphometry (VBM), and of microstructural modifications of the WM by means of Tract-Based Spatial Statistics (TBSS), as well as possible correlations with neuropsychological scores.

2 | MATERIAL AND METHODS

2.1 | Participants

From October 2015 to May 2016, 32 patients with genetically proven FD and 35 healthy controls (HC) of comparable age and sex were enrolled. To avoid the confounding effect of cerebrovascular events, participants with neither stroke nor transient ischemic attacks were not included in this study.

A subgroup of 20 FD patients underwent, within 1 week from the MR scan, a neuropsychological examination of different cognitive functions, including mini mental state evaluation (MMSE), Rey Auditory Verbal Learning Test (RAVLT), Corsi block-tapping test (CBTT), and attentional matrices (AM), as measures of general cognition, immediate and delayed verbal memory, visual memory, and attention, respectively.

Demographic and clinical information of enrolled subjects are listed in Table 1.

2.2 | Standard protocol approvals, registrations, and patient consents

This study was approved by the local Ethics Committee, and all subjects gave informed written consent.

TABLE 1 Participants' demographic and clinical variables

	HC	FD
Age (mean ± SD)	42.1 ± 14.5 (range 19–70)	43.3 ± 12.2 (range 20–68)
Sex (M/F)	14/21	12/20
ERT	n/a	29/32
ERT duration (mean ± SD)	n/a	48.9 ± 50.1
Hyposmia	n/a	3/32
Hypertension	n/a	8/32
Arrhythmia	n/a	1/32
Left ventricular hypertrophy	n/a	23/32
Renal failure	n/a	12/32
Proteinuria	n/a	10/32
Nicotine dependence	n/a	4/32
Acroparesthesia	n/a	22/32
Neuropathy	n/a	22/32
Cornea Verticillata	n/a	29/32
Angiocheratoma	n/a	30/32

2.3 | MRI data acquisition

MRI studies were performed on a 3 Tesla MRI scanner (Trio, Siemens Medical Systems, Erlangen, Germany). The following sequences were acquired in all subjects: a FLAIR sequence used for the assessment of the WM hyperintensities (WMH) load (TR = 6,000 ms; TE = 396 ms; TI = 2,200 ms; Flip Angle = 120°; voxel size = 1 × 1 × 1 mm^3; 160 sagittal slices); a structural T1w volumes acquired using a three-dimensional Magnetization-Prepared RApid Gradient-Echo sequence (MPRAGE; TR = 1,900 ms; TE = 3.4 ms; TI = 900 ms; Flip Angle = 9°; voxel size = 1x1x1 mm^3; 160 axial slices) for the assessment of brain atrophy using a VBM analysis; T2*-weighted volumes acquired using an echo-planar imaging sequence (TR = 2,500 ms; TE = 40 ms; 64 × 64 acquisition matrix; voxel size = 3 × 3 × 4 mm^3; gap 1 mm; 200 time points; 30 axial slices) used for the RS-fMRI analysis.

Furthermore, in all HC and in 20 FD patients DTI data were acquired using an echo-planar imaging sequence (TR = 7,400 ms; TE = 88 ms, 64 directions uniformly distributed in three dimensional space; B-factors 0 and 1,000 s/mm^2, 9 B0 images equally spaced throughout the DTI acquisition, voxel size = 2.2 × 2.2 × 2.2 mm^3, 60 axial slices) for the TBSS analysis.

2.4 | MRI data analysis

The load of WMH was rated according to a recent multicenter MR study on FD (Fazekas et al., 2015), summing two scores, each ranging from 0 to 3, respectively, for WMH in periventricular and deep hemispheric WM.

For the VBM analysis, structural data were processed using the Statistical Parametric Mapping (SPM8) software package (http://www.fil.ion.ucl.ac.uk/spm).

To assess differences in GM volume between the two groups, normalized GM maps were obtained from the unified segmentation tool (Ashburner & Friston, 2005) coupled to fast diffeomorphic registration algorithm (Diffeomorphic Anatomical Registration using Exponentiated Lie algebra; DARTEL) (Ashburner, 2007), using the default parameters. GM maps were then modulated by the Jacobian determinants, which were derived from the spatial normalization procedure, in order to preserve the local GM volumes. Images were then smoothed using a 6 mm FWHM isotropic Gaussian kernel, to reduce confounding effects derived by individual variations in gyral anatomy, and also to render the data more normally distributed as per the Gaussian random field model underlying the statistical process used for adjusting *p*-values. Finally, for each study total intracranial volume was calculated on the non-normalized segmented volumes as the number of voxels where the sum of the three segmented tissues probabilities (GM, WM, and CSF) exceeded 50%.

TBSS analysis was performed using FSL v. 5.0.9 (FMRIB's Software Library, www.fmrib.ox.ac.uk/fsl). DTI datasets were preliminarily corrected for head movements and eddy current distortions using eddy_correct (Smith et al., 2004), and diffusion sensitizing gradient directions were corrected according to the corresponding deformation vectors (Leemans & Jones, 2009). Subsequently, for each study a brain mask was obtained from the B0 images using the Brain Extraction Tool routine (Smith, 2002), and a diffusion-tensor model was fitted at each brain voxel to generate fractional anisotropy (FA) maps. FA volumes of all subjects were then aligned to a common target in the MNI 152 standard space (FMRIB58_FA) using a nonlinear registration procedure (FSL FNIRT), and interpolated to a voxel size of $1 \times 1 \times 1$ mm^3. Normalized FA maps were then visually assessed to ensure good quality of the normalization, and a WM "skeleton," representing alignment-invariant tracts in common to all subjects, was generated for the study data set applying a thinning algorithm to the average FA map, thresholded at 0.2 (Smith et al., 2006). Finally, FA maps of each subject were projected onto this skeleton for the statistical analysis.

RS-fMRI data were processed using the FC toolbox (CONN, v. 16.a, McGovern Institute for Brain Research, Massachusetts Institute of Technology, http://www.nitrc.org/projects/conn), which contains libraries for fMRI analysis based on SPM8.

Preprocessing steps included the removal of the first five time points (to allow for instability of the initial MRI signal), leaving 195 time points, motion correction, slice timing correction, and temporal despiking with a hyperbolic tangent squashing function to limit outlier values, followed by band-pass filtering ($0.008\ \text{Hz} < f < 0.09\ \text{Hz}$) and spatial smoothing (using a 6-mm Gaussian kernel). The motion correction procedure realigns the volumes of each study to the first one, iteratively finding the translation and rotation parameters that minimize a least-squares cost function derived from the voxel-by-voxel intensity differences from the reference image. This approach proved to be accurate in realigning fMRI volumes for motion correction purposes (Ardekani, Bachman, & Helpern, 2001).

From the motion correction procedure, the mean displacement of the brain voxels was computed as root-mean-square (RMS) (Van Dijk, Sabuncu, & Buckner, 2012) of the translations along the three axes. Studies with a mean relative RMS of 0.15 mm or higher, or with more than 1.5 mm displacement along or 1.5° rotation around any axis were discarded. Furthermore, a "scrubbing" procedure was applied (Power, Barnes, Snyder, Schlaggar, & Petersen,, 2012) to the time points, along with the preceding and the two following ones, that showed a framewise differential of signal intensity >9 *z*-values, to further suppress the effect of patient movements.

Resulting data sets were then normalized to the standard Montreal Neurological Institute (MNI) EPI template and resampled to a voxel size of $2 \times 2 \times 2$ mm^3. All images were visually assessed by an experienced operator (MQ), to evaluate the overall accuracy of the processing.

For each subject, BOLD signal time course was calculated separately for each of the main hubs of the DMN, namely the posterior cingulate and the ventral portion of the precuneus (PCC), the medial prefrontal cortex (MPFC), the right (RPL) and left (LPL) inferior parietal lobules, and the right and left medial temporal lobes (MTL). Therefore, these 6 structures were sampled using four spherical ROIs [spheres with 6 mm radius centered on PCC, MPFC, RPL, and LPL (Fox et al., 2005)], and the hyppocampal ROIs from the Harvard-Oxford Atlas (Desikan et al., 2006), all available in CONN.

For each ROI, corresponding correlation map of the BOLD signal across the brain was generated, including in a General Linear Model (GLM) the time courses of WM and CSF signals, and the six parameters (translations and rotations along the X, Y, and Z axes) of spatial transformation, as derived from the coregistration step.

2.5 | Statistical analysis: Group differences

Differences between FD and HC groups in terms of age and sex were probed by Student *t*-test and Chi-squared test, respectively.

For the VBM analysis, the normalized GM maps were statistically analyzed to assess local differences between the two groups in GM volume using the GLM, including age and sex and total intracranial volume as confounding variable (the latter entered in the model to normalize for head size). Differences were considered significant for $p < .05$, corrected for family wise error at cluster level.

For the TBSS, skeletonized FA maps were fed into a voxel-wise cross-subject nonparametric analysis based on permutations applied to the GLM (Bullmore et al., 1999), including age and sex as nuisance covariate (number of permutations = 5,000). Results were considered significant at $p < .05$, corrected for multiple comparisons at a cluster level using the threshold-free cluster enhancement approach (Smith et al., 2006).

For the RS-fMRI analysis, FC maps of the two groups were statistically analyzed to test for possible differences in the FC of the six seeds, including age and sex and the average RMS of the translation parameters as confounding variable in a GLM (the latter entered in the model to remove potential residual movement effects). Differences were considered significant for $p < .008$ (0.05 Bonferroni corrected, considering

that 6 ROIs were tested separately), corrected for the family wise error at cluster level.

For all analyses, both contrasts (i.e., HC > FD and HC > FD) were tested when probing between-group differences.

2.6 | Statistical analysis: Correlations between MR and clinical data

When significant differences between groups emerged at imaging, possible correlations between clinical scores and MRI data were tested voxel-wise.

For VBM and TBSS, both direct and inverse correlations with clinical scores (MMSE, RAVLT, CBTT, and AM) were tested voxel-wise using the same GLM approach (parametric for VBM, and non-parametric for TBSS) as for between-group differences. Results were considered significant at $p < .01$ (0.05 Bonferroni-corrected for five tested clinical scores).

Similarly, possible correlations between the FC of the six hubs of the DMN with the clinical scores were also tested voxel-wise using the same approach as for between-group differences, with a significance level for $p < .0016$ (0.05 Bonferroni-corrected for 30 test, as FC with six seeds was probed for correlation with five clinical scores).

2.7 | Statistical analysis: Correlations between imaging techniques

When significant differences between groups emerged at imaging, possible correlations between different techniques were tested cluster-wise. To this end, for each significant cluster the corresponding first eigenvariate (for VBM and RS-fMRI) or mean value (for TBSS) was extracted, and their relationships were assessed pairwise by partial correlation analysis, including as nuisance age, sex, and mean motion.

Significance level was set to 0.05, Bonferroni-corrected for multiple comparisons.

3 | RESULTS

The FD and HC groups were not significantly different for age and sex.

Mean ± standard deviation scores of the neuropsychological tests in the FD group were: 28.5 ± 2.0 for the MMSE, 42.1 ± 9.8 for the RAVLT immediate, 8.4 ± 3.4 for the RAVLT delayed, 5.0 ± 0.9 for the CBTT, and 50.5 ± 7.6 for the AM.

The analysis of the WMH load showed that 56.2% of FD patients (18/32 subjects) scored a Fazekas' score of 0, with no significant WMH both in periventricular and deep hemispheric regions. Among the remaining 14 patients, 11 subjects scored 1 in the evaluation of the deep WMH, 2 patients scored 1 for both deep and periventricular WMH, and only one subject (3.1% of the total FD patients) showed a high WMH load, scoring 3 for both WM locations.

The VBM analysis did not show any significant cluster of decreased or increased GM density in FD patients.

At TBSS analysis, a single extensive cluster of reduced FA across the WM skeleton was present, mainly involving major commissural tracts, with relative sparing of temporal and occipital lobes bilaterally, genu and splenium of corpus callosum, and cerebellar fibers on the left hemisphere (Figure 1).

Five FD patients and two HC were excluded from the RS-fMRI analysis because of excessive movements during the fMRI scan. In the remaining 60 studies, the difference in the RMS (0.031 ± 0.017 in HC and 0.044 ± 0.034 in FD), as well as in age (mean age 41.4 ± 14.5 in HC and 43.3 ± 12.0 in FD) and sex (13 M and 20 F in HC; 11 M and 16 F in FD) were not significant between the two groups.

The results of the between-group RS-fMRI analysis are shown in Figure 2 and listed in Table 2.

When evaluating the MPFC seed, clusters of significantly increased FC in FD emerged in the medial orbitofrontal cortex, in superior frontal and middle temporal gyri bilaterally, in the left angular gyrus, and in the right superior parietal lobule, as well as in the right cerebellar hemisphere, mainly involving Crus 2.

When evaluating the PCC seed, a single cluster of increased FC emerged in the right angular gyrus.

When evaluating the RPL seed, clusters of significant FC increase were observed in the left paracingulate gyrus extending into the MPFC and in the left superior frontal gyrus, as well as in the right cerebellar hemisphere (Crus 1 and Crus 2).

No significant differences between the two groups emerged for the remaining seeds (namely LPL, right and left MTL), or when probing the HC > FD contrast for any of the tested seeds.

When testing the relationships of TBSS and RS-fMRI data with clinical scores (VBM analysis did not result in any significant cluster of GM volume differences between groups), no correlation emerged with FA as assessed by TBSS, while a direct correlation between the right inferior frontal gyrus and the CBTT emerged at RS-fMRI when testing the PCC seed ($p = .0001$; Figure 3). No other significant correlation was found for any of the remaining seeds with the other clinical scores.

Finally, when testing the relationship between TBSS results and FC modifications in the group of 16 FD patients included in both the RS-fMRI and DTI analyses, a significant inverse correlation between mean FA and regions of altered FC with RPL emerged ($p = .003$; $R = -0.759$), while the clusters of increased connectivity with MPFC and PCC did not show significant associations with TBSS.

4 | DISCUSSION

In FD patients, we found clusters of increased FC with DMN hubs, involving both cerebral and cerebellar cortical regions, and partially correlated to the extensive WM microstructural alterations demonstrated in these subjects at TBSS. Furthermore, the FC between the precuneus and the right inferior frontal gyrus showed a significant correlation with the scores obtained at the CBTT.

While CNS pathology in FD mainly consists of cerebral vasculopathy, that ranges from stroke to clinically asymptomatic WMH (Kolodny et al., 2015), mild neuropsychological symptoms are relatively common in these patients (Bolsover et al., 2014; Fellgiebel, Muller, & Ginsberg, 2006b). Indeed, depression has been reported in up to 50%

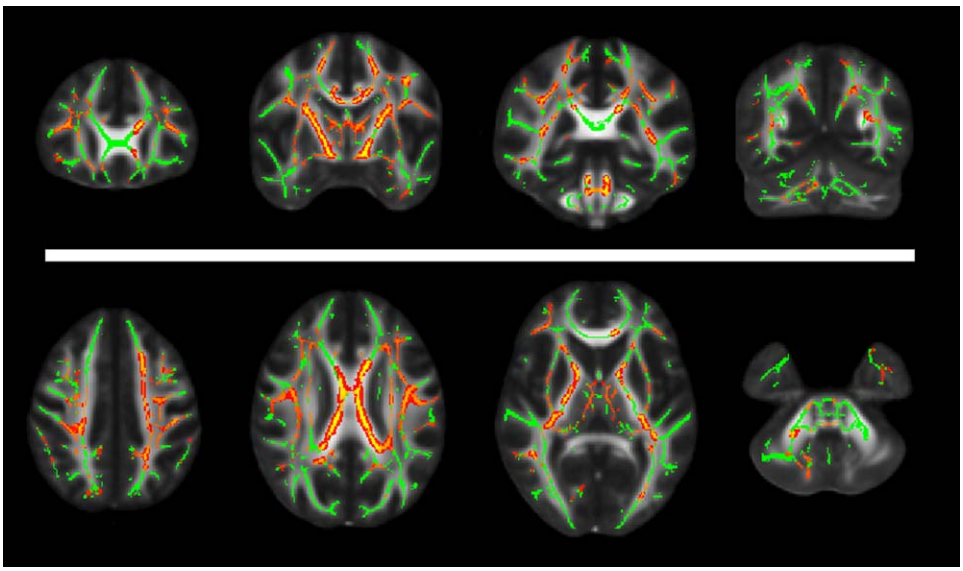

FIGURE 1 Results of the TBSS analysis superimposed to the FA template in the standard MNI space for anatomic reference. In the upper row, from left to right, selected coronal slices at the level of the genu of the corpus callosum, body of the corpus callosum and internal capsule, splenium of the corpus callosum and brainstem, and of the occipital lobe and cerebellar hemispheres, respectively. In the lower row, from left to right, axial slices are shown at the level of the centrum semiovale, corpus callosum, internal capsule, and cerebellum, respectively [Color figure can be viewed at wileyonlinelibrary.com]

of FD patients (Cole et al., 2007), and impairment in other domains (i.e., executive functioning, information processing speed and attention) has been described, with a preservation of global cognitive functioning (Bolsover et al., 2014).

In our study, FD patients showed normal results at the MMSE, AM, CBTT, and RAVLT immediate score. In contrast, RAVLT delayed results were below the mean values reported in the Italian population (Carlesimo et al., 2012), indicating an isolated impairment of long-term verbal memory. This is in contrast with previous reports where normal memory and impaired attention was observed in FD (Schermuly et al., 2011). However, that group of patients differed from the present population, as patients with previous cerebrovascular events were also included (Schermuly et al., 2011). Future studies with more extensive neuropsychological batteries are needed to better depict the cognitive impairment of FD patients.

According to previous volumetric studies (Cocozza et al., 2017; Paavilainen et al., 2013), no major regional GM alterations are present in FD, with our VBM analysis substantially replicating these results.

On the contrary, WM damage has been previously detected in this condition, and has been largely attributed to microvascular pathology due to Gb-3 accumulation in vascular cells (endothelial and smooth muscle cells). This accumulation causes tissue injuries that are likely to correspond to the hyperintensities seen in the WM of these patients on T2w images (Kolodny et al., 2015). Beside these discrete WM lesions, several DTI studies have demonstrated that in FD a more extensive pattern of microstructural damage is present, somewhat

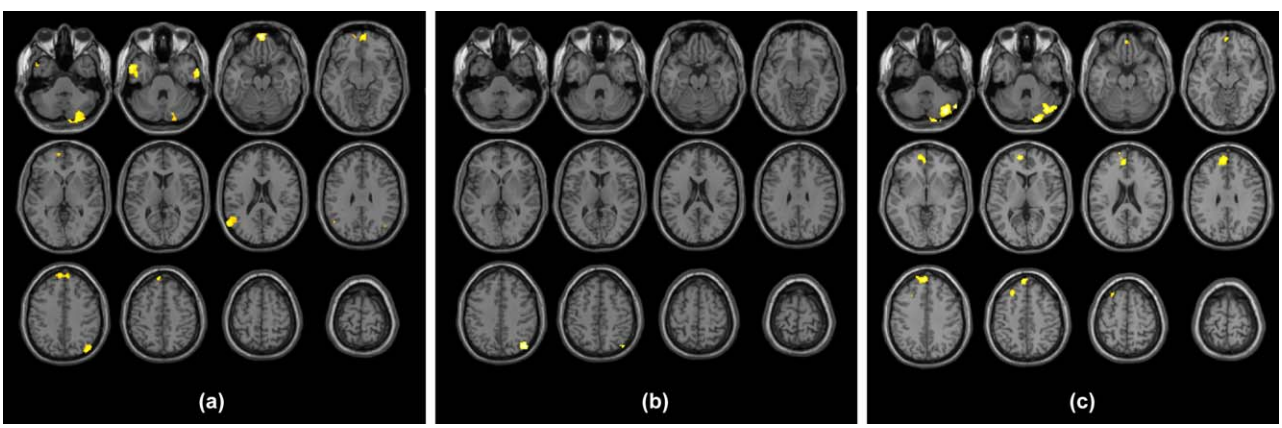

FIGURE 2 Clusters resulting from the FD > HC between-group contrast for the seed placed at level of the MPFC (a), of the ventral portion of the precuneus (b), and of the right parietal lobule (c). Results are superimposed for anatomic reference to a single individual's T1-weighted volume in the standard MNI space, with subject's right at the observer's right. Significance for all clusters is $p < .008$, family wise error corrected at cluster level [Color figure can be viewed at wileyonlinelibrary.com]

TABLE 2 Results of the second-level analysis of RS-fMRI data

				MNI Coordinates (mm)			
Seed	**Cluster volume (mL)**	***p*-value**	***T***	***X***	***Y***	***Z***	
MPFC	4.3	<.0001	5.24	26	−90	−36	Right Cerebellum (Lobule VIIa Crus II)
			3.71	20	−80	−30	Right Cerebellum (Lobule VIIa Crus I)
	4.0	<.0001	6.11	0	62	−20	Left Rectal Gyrus
			4.74	4	62	−6	Right Mid Orbital Gyrus
			3.90	−10	58	−4	Left Mid Orbital Gyrus
			3.64	−14	64	−14	Left Superior Orbital Gyrus
	3.1	.0001	5.26	−56	4	−30	Left Middle Temporal Gyrus
			4.86	−50	8	−34	Left Medial Temporal Pole
			4.56	−48	−10	−28	Left Inferior Temporal Gyrus
	2.7	.0003	5.24	−8	58	36	Left Superior Frontal Gyrus
	2.6	.0004	4.59	−48	−64	24	Left Angular Gyrus
			3.83	−48	−56	20	Left Middle Temporal Gyrus
	1.8	.004	5.31	64	−2	−28	Right Middle Temporal Gyrus
	1.7	.006	4.41	46	−76	40	Right Angular Gyrus
			3.38	42	−68	32	Right Middle Occipital Gyrus
PCC	2.1	.001	4.93	44	−74	42	Right Angular Gyrus
RPL	9.8	<.0001	5.32	−12	58	4	Left Superior Frontal Gyrus
			4.26	−4	54	−4	Left Mid Orbital Gyrus
			3.56	2	50	−20	Right Rectal Gyrus
	9.6	<.0001	5.63	36	−76	−36	Right Cerebellum (Lobule VIIa Crus I)
			5.04	18	−94	−32	Right Cerebellum (Lobule VIIa Crus II)
	1.6	.007	4.20	−26	30	48	Left Middle Frontal Gyrus

independent from conventional MRI-detectable WMH, and predominantly distributed to deep and periventricular WM, probably due to microangiopathic alterations mainly affecting the long perforating arteries (Albrecht et al., 2007; Fellgiebel et al., 2006a; Paavilainen et al., 2013). In line with these results, in our TBSS analysis FD patients showed, despite a low incidence and load of WMH, a relatively widespread alteration of WM integrity, compared to HC, confirming the sensitivity of DTI measures in detecting and quantifying microstructural brain tissue alterations, even in normal-appearing WM on conventional MR images. The exact pathogenesis of WM damage in FD is, however, not completely known. Indeed, the subtle and pervasive pattern of WM involvement demonstrated in our study slightly differs from what has been observed in other forms of cerebral small vessel disease (CSVD; Pasi, van Uden, Tuladhar, de Leeuw, & Pantoni, 2016; Wardlaw, Smith, & Dichgans, 2013), thus highlighting the differences between Fabry's microangiopathy and common sporadic CSVD, or even suggesting that additional, not purely vascular, mechanisms could play a role in determining WM injury in this condition.

The DMN is a set of functionally interconnected brain areas, characterized by greater activation during rest, with intrinsic functions related to internal mentation (Andrews-Hanna, 2012). In recent years, it has gained particular attention, emerging as the most studied and well-described resting-state network, mainly due to its apparently central role in the coordination of sensori-motor and cognitive goal-directed activities, with specific alterations of the DMN reported as a hallmark of numerous neurological and psychiatric diseases (Buckner, Andrews-Hanna, & Schacter, 2008).

The variable association of executive dysfunction and depression with the relatively widespread involvement of deep and periventricular WM is present also in other chronic, although etiopathogenetically different, conditions, such as sporadic CSVD, multiple sclerosis (MS), late-life depression (LLD), and mild cognitive impairment (MCI). However, the exact nature and the causal chain of this relationship have not been fully understood yet (Delano-Wood et al., 2008; Schermuly et al., 2011; Sexton et al., 2012).

Different DMN changes have been described in the above mentioned conditions. In MCI patients with CSVD, a task-induced deactivation study demonstrated impaired deactivation of the precuneus/PCC hub of the DMN during the execution of a cognitive task (Papma et al., 2014). Furthermore, DTI showed CSVD-related microstructural damage in fiber tracts subserving the DMN in these subjects, supporting the hypothesis that alterations of WM integrity affect cognition through

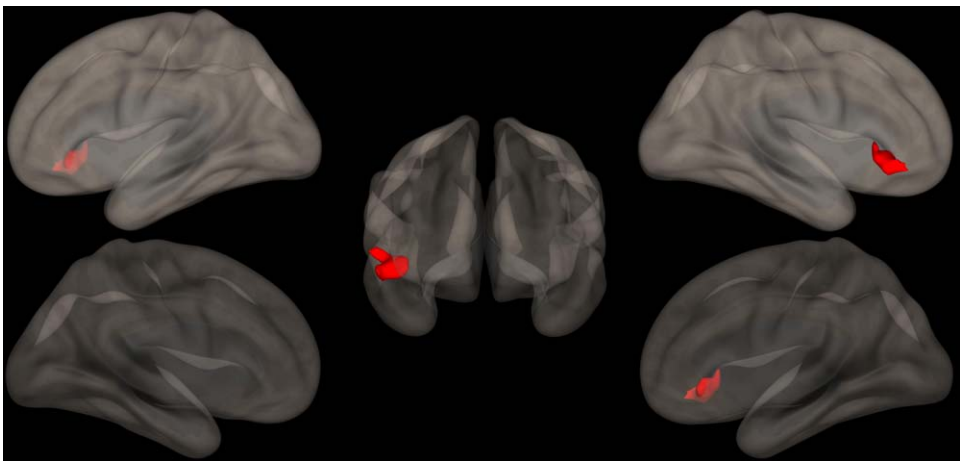

FIGURE 3 Direct correlations between the FC of the precuneus and the scores at the CBTT. A cluster of significantly correlated FC ($p = .0001$) is evident at the level of right inferior frontal gyrus, superimposed on the 3-dimensional rendering of a healthy brain in the MNI space. ERT: enzyme replacement therapy; FD: Fabry disease; HC: healthy control; n/a: not applicable. Ages are expressed in years, while ERT duration is expressed in months. Renal failure considered present when the estimated glomerular filtration rate of the patient was < 90 mL/min (no patient had end-stage renal disease requiring dialysis), while proteinuria was considered present when the patient scored a value > 150 mg/24 hr. MPFC: medial prefrontal cortex; PCC: ventral portion of the precuneus; RPL: right parietal lobule; MNI: Montreal Neurological Institute. Anatomic labeling is according to Tzourio-Mazoyer et al. (2002) [Color figure can be viewed at wileyonlinelibrary.com]

interference with network functioning (Papma et al., 2014; Teipel et al., 2010). Furthermore, in LLD, an RS-fMRI study demonstrated decreased FC between the subgenual ACC (sACC) and the PCC, as well as an increased FC between the PCC and both the dorso-MPFC and the orbito-frontal cortex, with a significant inverse correlation between WMH volume and RS-fMRI connectivity in the MPFC hub of the DMN (Wu et al., 2011). These results, coupled to the reported inverse correlation between the anisotropy of frontal fiber tracts, subserving the anterior hub of the DMN, and the impairment in the executive functioning and processing speed domains, support the role of WM microstructural damage in hampering frontal-striatal-limbic networks in LLD (Alexopoulos, Kiosses, Choi, Murphy, & Lim, 2002; Sexton et al., 2012). Finally, a dysfunction of the anterior components of the DMN has been demonstrated in patients with primary progressive MS, with FC in the left medial PFC (mPFC), the left precentral gyrus (PcG) and the ACC, correlating with cognitive impairment and integrity of the corpus callosum and cingulum, again supporting the hypothesis of a disruption of fiber bundles interconnecting different DMN hubs as the predisposing condition for FC alterations and cognitive impairment (Rocca et al., 2010).

Contrary to the pattern of reduced DMN FC observed in these other pathologies, in our patients we found clusters of increased connectivity to three hubs of the DMN, located both in cortical regions known to be part of the DMN itself (e.g., medial frontal cortex, precuneus and parietal cortices bilaterally) or clearly outside of it (e.g., cerebellar Crus I and Crus II). Moreover, no clusters of reduced FC were found in FD patients compared with HC.

Increased FC in cortical areas implicated in the DMN has been previously reported in other conditions such as early stages of MS, Clinically Isolated Syndrome and mild traumatic brain injury, which share with FD a diffuse, although mild, involvement of WM (Hawellek, Hipp, Lewis, Corbetta, & Engel, 2011; Newsome et al., 2016; Roosendaal et al., 2010; Sharp et al., 2011).

Two different mechanisms could generate this increased connectivity in conditions where a diffuse reduction of structural connectivity, more than the complete disruption of specific connections, represents the prevalent feature: a maladaptive mechanism or a compensatory one. The first mechanism ensues from the loss of diversity and flexibility in large scale cortical interactions derived from widespread reduction in WM integrity, which may result in a preferential participation in more global patterns of activity, such as the DMN (Hawellek et al., 2011). Alternatively, increased FC could reflect a functional reorganization of the cortex due to neural plasticity with the aim of functionally compensating the underlying WM damage (Hawellek et al., 2011; Sharp et al., 2011).

Therefore, it is reasonable to hypothesize that only in more advanced phases of the disease, with WM alterations becoming more extensive, a further disruption of WM circuits could lead to an exhaustion of the cortical functional reserve capacity and a reduction of FC within the DMN also in FD, as it happens in other conditions (Rocca et al., 2010; Teipel et al., 2010). Indeed, subjects with major cerebrovascular events were not included in our study and FD patients showed a low incidence and load of WMH.

Furthermore, we found increased connectivity between different nodes of the DMN and cortical regions not typically involved in the DMN, or even implicated in other resting-state networks whose function is known to be functionally anticorrelated to the DMN itself, such as Crus I and Crus II (Fox et al., 2005; Uddin, Kelly, Biswal, Castellanos, & Milham, 2009). Again, this finding could reflect a maladaptive condition of weakening, or even of loss, of the physiological anticorrelation between the DMN and other resting-state networks or, most likely, it could be the expression of a recruiting mechanism, as a part of the

cortical functional compensation effort. Finally, it should be noted that in FD patients an higher incidence of microbleeds has been reported (Kono et al., 2016; Reisin et al., 2011), with a known influence on both functional and structural connectivity (Akoudad et al., 2013; Sharp et al., 2011). However, in our population T2*-GrE images were available, and no microbleeds were found, thus allowing us to discard the hypothesis of connectivity changes due to the presence of this alteration (data not shown).

When analyzing the relationship between MR and clinical data, we found no significant correlation between measures of WM integrity all over the brain and neuropsychological scores. This lack of correspondence between WM alterations and clinical performance could, once more, be explained by the reserve capacity of cortical function, which is able to compensate for initial and relatively mild WM damage. However, when investigating the relationship between neuropsychological tests and resting-state connectivity, we found that FC between right inferior frontal gyrus and precuneus significantly correlated with the results obtained at the CBTT. Although this finding is in line with some previous lesion-mapping and task-related fMRI studies, which highlight the importance of the right prefrontal cortex as a neural substratum of spatial working memory (Nemmi, Boccia, Piccardi, Galati, & Guariglia, 2013; Toepper et al., 2014; van Asselen et al., 2006), further studies are needed to elucidate the mechanisms underlying this correlation, which does not specifically involve the dorso-lateral prefrontal cortex, known to play a central role in spatial working memory (Nemmi et al., 2013; Toepper et al., 2014; van Asselen et al., 2006).

Finally, we explored possible correlations in FD patients between FC of the regions of significantly altered connectivity and global measures of microstructural damage, showing a significant inverse correlation between WM integrity and alterations of FC with RPL. Of note, this finding further supports the previously generated hypotheses according to which a mild, although diffuse, WM damage is balanced by a proportional increase in FC either by maladaptive or compensatory mechanisms. Interestingly, we did not find correlations between TBSS alterations and FC alterations of the midline hubs of the DMN, although it should be considered that the limited number of subjects for whom both DTI and RS-fMRI data were available may have limited our sensitivity to this correlation.

Further limitations of this study are the low incidence and load of WMH in our patients, and the ongoing enzyme replacement therapy in most patients, that both could lead to an underestimation of the real impact of FD on brain structure and function, thus again limiting the sensitivity of our analysis.

5 | CONCLUSION

In FD increased FC with several DMN hubs is present, involving both supratentorial and infratentorial structures, correlated to the widespread WM microstructural alterations present in this condition. Furthermore, these FC increases appear to partially correlate with the patients' cognitive status. Taken together, these results confirm and expand the current knowledge about the cerebral involvement in these patients, supporting the hypothesis that FD should not be considered only as a disease in which major cerebrovascular events develop, but also as a condition in which significant and diffuse microstructural and functional changes occur, at least partially independently from cerebral vasculopathy.

AUTHORS' CONTRIBUTIONS

Sirio Cocozza: Study conception and design; Analysis and interpretation
Giuseppe Pontillo: Study conception and design; Analysis and interpretation
Mario Quarantelli: Analysis and interpretation; Critical Revision
Francesco Saccà: Acquisition of data; Analysis and interpretation
Eleonora Riccio: Acquisition of data
Teresa Costabile: Acquisition of data
Gaia Olivo: Acquisition of data
Vincenzo Brescia Morra: Analysis and interpretation
Antonio Pisani: Acquisition of data; Critical Revision
Arturo Brunetti: Critical Revision; Study Supervision
Enrico Tedeschi: Critical Revision; Study Supervision

ACKNOWLEDGMENT

Dr. Cocozza reports fees for speaking by Genzyme. Dr. Pontillo, Dr. Quarantelli, Dr. Saccà, Dr. Riccio, Dr. Costabile, Dr. Olivo, Dr. Brescia Morra, and Dr. Brunetti reports no disclosures. Dr. Pisani received reimbursement for attending symposiums, fees for speaking, funds for research and fees for consulting by Shire, Genzyme and Amicus companies. Dr. Tedeschi received fees for consulting by Shire, Ars Educandi and Scientific Press companies.

ORCID

Sirio Cocozza http://orcid.org/0000-0002-0300-5160
Giuseppe Pontillo http://orcid.org/0000-0001-5425-1890
Mario Quarantelli http://orcid.org/0000-0001-7836-454X

REFERENCES

Akoudad, S., de Groot, M., Koudstaal, P. J., van der Lugt, A., Niessen, W. J., Hofman, A., ... Vernooij, M. W. (2013). Cerebral microbleeds are related to loss of white matter structural integrity. *Neurology*, *81*, 1930–1937.

Albrecht, J., Dellani, P. R., Muller, M. J., Schermuly, I., Beck, M., Stoeter, P., ... Fellgiebel, A. (2007). Voxel based analyses of diffusion tensor imaging in Fabry disease. *Journal of Neurology, Neurosurgery, & Psychiatry*, *78*, 964–969.

Alexopoulos, G. S., Kiosses, D. N., Choi, S. J., Murphy, C. F., & Lim, K. O. (2002). Frontal white matter microstructure and treatment response of late-life depression: A preliminary study. *American Journal of Psychiatry*, *159*, 1929–1932.

Andrews-Hanna, J. R. (2012). The brain's default network and its adaptive role in internal mentation. *The Neuroscientist: A Review Journal Bringing Neurobiology, Neurology and Psychiatry*, *18*, 251–270.

Ardekani, B. A., Bachman, A. H., & Helpern, J. A. (2001). A quantitative comparison of motion detection algorithms in fMRI. *Magnetic Resonance Imaging*, *19*, 959–963.

Argyelan, M., Ikuta, T., DeRosse, P., Braga, R. J., Burdick, K. E., John, M., … Szeszko, P. R. (2014). Resting-state fMRI connectivity impairment in schizophrenia and bipolar disorder. *Schizophrenia Bulletin*, *40*, 100–110.

Ashburner, J. (2007). A fast diffeomorphic image registration algorithm. *Neuroimage*, *38*, 95–113.

Ashburner, J., & Friston, K. J. (2005). Unified segmentation. *Neuroimage*, *26*, 839–851.

Bolsover, F. E., Murphy, E., Cipolotti, L., Werring, D. J., & Lachmann, R. H. (2014). Cognitive dysfunction and depression in Fabry disease: a systematic review. *Journal of Inherited Metabolic Disease*, *37*, 177–187.

Buckner, R. L., Andrews-Hanna, J. R., & Schacter, D. L. (2008). The brain's default network: Anatomy, function, and relevance to disease. *Annals of the New York Academy of Sciences*, *1124*, 1–38.

Bullmore, E. T., Suckling, J., Overmeyer, S., Rabe-Hesketh, S., Taylor, E., & Brammer, M. J. (1999). Global, voxel, and cluster tests, by theory and permutation, for a difference between two groups of structural MR images of the brain. *IEEE Transactions on Medical Imaging*, *18*, 32–42.

Carlesimo, G. A., Piras, F., Assogna, F., Pontieri, F. E., Caltagirone, C., & Spalletta, G. (2012). Hippocampal abnormalities and memory deficits in Parkinson disease: a multimodal imaging study. *Neurology*, *78*, 1939–1945.

Cataldi, M., Avoli, M., & de Villers-Sidani, E. (2013). Resting state networks in temporal lobe epilepsy. *Epilepsia*, *54*, 2048–2059.

Cocozza, S., Pisani, A., Olivo, G., Sacca, F., Ugga, L., Riccio, E., … Tedeschi, E. (2017). Alterations of functional connectivity of the motor cortex in Fabry disease: An RS-fMRI study. *Neurology*, *88*, 1822–1829.

Cole, A. L., Lee, P. J., Hughes, D. A., Deegan, P. B., Waldek, S., & Lachmann, R. H. (2007). Depression in adults with Fabry disease: A common and under-diagnosed problem. *Journal of Inherited Metabolic Disease*, *30*, 943–951.

Delano-Wood, L., Abeles, N., Sacco, J. M., Wierenga, C. E., Horne, N. R., & Bozoki, A. (2008). Regional white matter pathology in mild cognitive impairment: Differential influence of lesion type on neuropsychological functioning. *Stroke*, *39*, 794–799.

Desikan, R. S., Segonne, F., Fischl, B., Quinn, B. T., Dickerson, B. C., Blacker, D., … Killiany, R. J. (2006). An automated labeling system for subdividing the human cerebral cortex on MRI scans into gyral based regions of interest. *Neuroimage*, *31*, 968–980.

Dutta, A., McKie, S., & Deakin, J. F. (2014). Resting state networks in major depressive disorder. *Psychiatry Res*, *224*, 139–151.

Fazekas, F., Enzinger, C., Schmidt, R., Grittner, U., Giese, A. K., Hennerici, M. G., … Rolfs, A. (2015). Brain magnetic resonance imaging findings fail to suspect Fabry disease in young patients with an acute cerebrovascular event. *Stroke*, *46*, 1548–1553.

Fellgiebel, A., Mazanek, M., Whybra, C., Beck, M., Hartung, R., Muller, K. M., … Muller, M. J. (2006a). Pattern of microstructural brain tissue alterations in Fabry disease: A diffusion-tensor imaging study. *Journal of Neurology*, *253*, 780–787.

Fellgiebel, A., Muller, M. J., & Ginsberg, L. (2006b). CNS manifestations of Fabry's disease. *The Lancet. Neurology*, *5*, 791–795.

Fox, M. D., Snyder, A. Z., Vincent, J. L., Corbetta, M., Van Essen, D. C., & Raichle, M. E. (2005). The human brain is intrinsically organized into dynamic, anticorrelated functional networks. *Proceedings of the National Academy of Sciences of the United States of America*, *102*, 9673–9678.

Germain, D. P. (2010). Fabry disease. *Orphanet Journal of Rare Diseases*, *5*, 30.

Hawellek, D. J., Hipp, J. F., Lewis, C. M., Corbetta, M., & Engel, A. K. (2011). Increased functional connectivity indicates the severity of cognitive impairment in multiple sclerosis. *Proceedings of the National Academy of Sciences of the United States of America*, *108*, 19066–19071.

Kolodny, E., Fellgiebel, A., Hilz, M. J., Sims, K., Caruso, P., Phan, T. G., … Burlina, A. (2015). Cerebrovascular involvement in Fabry disease: Current status of knowledge. *Stroke*, *46*, 302–313.

Kono, Y., Wakabayashi, T., Kobayashi, M., Ohashi, T., Eto, Y., Ida, H., & Iguchi, Y. (2016). Characteristics of Cerebral Microbleeds in Patients with Fabry Disease. *Journal of Stroke Cerebrovascular Disease*, *25*, 1320–1325.

Leemans, A., & Jones, D. K. (2009). The B-matrix must be rotated when correcting for subject motion in DTI data. *Magnetic Resonance in Medicine*, *61*, 1336–1349.

Nemmi, F., Boccia, M., Piccardi, L., Galati, G., & Guariglia, C. (2013). Segregation of neural circuits involved in spatial learning in reaching and navigational space. *Neuropsychologia*, *51*, 1561–1570.

Newsome, M. R., Li, X., Lin, X., Wilde, E. A., Ott, S., Biekman, B., … Levin, H. S. (2016). Functional connectivity is altered in concussed adolescent athletes despite medical clearance to return to play: A preliminary report. *Frontiers in Neurology*, *7*, 116.

Paavilainen, T., Lepomaki, V., Saunavaara, J., Borra, R., Nuutila, P., Kantola, I., & Parkkola, R. (2013). Diffusion tensor imaging and brain volumetry in Fabry disease patients. *Neuroradiology*, *55*, 551–558.

Papma, J. M., de Groot, M., de Koning, I., Mattace-Raso, F. U., van der Lugt, A., Vernooij, M. W., … Smits, M. (2014). Cerebral small vessel disease affects white matter microstructure in mild cognitive impairment. *Human Brain Mapping*, *35*, 2836–2851.

Pasi, M., van Uden, I. W., Tuladhar, A. M., de Leeuw, F. E., & Pantoni, L. (2016). White matter microstructural damage on diffusion tensor imaging in cerebral small vessel disease: Clinical consequences. *Stroke*, *47*, 1679–1684.

Power, J. D., Barnes, K. A., Snyder, A. Z., Schlaggar, B. L., & Petersen, S. E. (2012). Spurious but systematic correlations in functional connectivity MRI networks arise from subject motion. *Neuroimage*, *59*, 2142–2154.

Prodoehl, J., Burciu, R. G., & Vaillancourt, D. E. (2014). Resting state functional magnetic resonance imaging in Parkinson's disease. *Current Neurology and Neuroscience Reports*, *14*, 448.

Quarantelli, M., Salvatore, E., Giorgio, S. M., Filla, A., Cervo, A., Russo, C. V., … De Michele, G. (2013). Default-mode network changes in Huntington's disease: an integrated MRI study of functional connectivity and morphometry. *PLoS One*, *8*, e72159.

Raichle, M. E. (2015). The brain's default mode network. *Annual Review of Neuroscience*, *38*, 433–447.

Reisin, R. C., Romero, C., Marchesoni, C., Napoli, G., Kisinovsky, I., Caceres, G., & Sevlever, G. (2011). Brain MRI findings in patients with Fabry disease. *Journal of the Neurological Sciences*, *305*, 41–44.

Rocca, M. A., Valsasina, P., Absinta, M., Riccitelli, G., Rodegher, M. E., Misci, P., … Filippi, M. (2010). Default-mode network dysfunction and cognitive impairment in progressive MS. *Neurology*, *74*, 1252–1259.

Roosendaal, S. D., Schoonheim, M. M., Hulst, H. E., Sanz-Arigita, E. J., Smith, S. M., Geurts, J. J., & Barkhof, F. (2010). Resting state networks change in clinically isolated syndrome. *Brain*, *133*, 1612–1621.

Schermuly, I., Muller, M. J., Muller, K. M., Albrecht, J., Keller, I., Yakushev, I., … Fellgiebel, A. (2011). Neuropsychiatric symptoms and brain structural alterations in Fabry disease. *European Journal of Neurology*, *18*, 347–353.

Sexton, C. E., McDermott, L., Kalu, U. G., Herrmann, L. L., Bradley, K. M., Allan, C. L., ... Ebmeier, K. P. (2012). Exploring the pattern and neural correlates of neuropsychological impairment in late-life depression. *Psychological Medicine*, *42*, 1195–1202.

Sharp, D. J., Beckmann, C. F., Greenwood, R., Kinnunen, K. M., Bonnelle, V., De Boissezon, X., ... Leech, R. (2011). Default mode network functional and structural connectivity after traumatic brain injury. *Brain*, *134*, 2233–2247.

Sims, K., Politei, J., Banikazemi, M., & Lee, P. (2009). Stroke in Fabry disease frequently occurs before diagnosis and in the absence of other clinical events: Natural history data from the Fabry Registry. Stroke, *40*, 788–794.

Smith, S. M. (2002). Fast robust automated brain extraction. *Human Brain Mapping*, *17*, 143–155.

Smith, S. M., Jenkinson, M., Johansen-Berg, H., Rueckert, D., Nichols, T. E., Mackay, C. E., ... Behrens, T. E. (2006). Tract-based spatial statistics: voxelwise analysis of multi-subject diffusion data. *Neuroimage*, *31*, 1487–1505.

Smith, S. M., Jenkinson, M., Woolrich, M. W., Beckmann, C. F., Behrens, T. E., Johansen-Berg, H., ... Matthews, P. M. (2004). Advances in functional and structural MR image analysis and implementation as FSL. *Neuroimage*, *23*(Suppl 1), S208–S219.

Teipel, S. J., Bokde, A. L., Meindl, T., Amaro, E., Jr., Soldner, J., Reiser, M. F., ... Hampel, H. (2010). White matter microstructure underlying default mode network connectivity in the human brain. *Neuroimage*, *49*, 2021–2032.

Toepper, M., Markowitsch, H. J., Gebhardt, H., Beblo, T., Bauer, E., Woermann, F. G., ... Sammer, G. (2014). The impact of age on prefrontal cortex integrity during spatial working memory retrieval. *Neuropsychologia*, *59*, 157–168.

Tzourio-Mazoyer, N., Landeau, B., Papathanassiou, D., Crivello, F., Etard, O., Delcroix, N., ... Joliot, M. (2002). Automated anatomical labeling of activations in SPM using a macroscopic anatomical parcellation of the MNI MRI single-subject brain. *Neuroimage*, *15*, 273–289.

Uddin, L. Q., Kelly, A. M., Biswal, B. B., Castellanos, F. X., & Milham, M. P. (2009). Functional connectivity of default mode network components: correlation, anticorrelation, and causality. *Human Brain Mapping*, *30*, 625–637.

van Asselen, M., Kessels, R. P., Neggers, S. F., Kappelle, L. J., Frijns, C. J., & Postma, A. (2006). Brain areas involved in spatial working memory. *Neuropsychologia*, *44*, 1185–1194.

Van Dijk, K. R., Sabuncu, M. R., & Buckner, R. L. (2012). The influence of head motion on intrinsic functional connectivity MRI. *Neuroimage*, *59*, 431–438.

Vemuri, P., Jones, D. T., & Jack, C. R. Jr. (2012). Resting state functional MRI in Alzheimer's Disease. *Alzheimer's Research & Therapy*, *4*, 2.

Wardlaw, J. M., Smith, C., & Dichgans, M. (2013). Mechanisms of sporadic cerebral small vessel disease: Insights from neuroimaging. *The Lancet Neurology*, *12*, 483–497.

Wu, M., Andreescu, C., Butters, M. A., Tamburo, R., Reynolds, C. F., III, & Aizenstein, H. (2011). Default-mode network connectivity and white matter burden in late-life depression. *Psychiatry Research*, *194*, 39–46.

How to cite this article: Cocozza S, Pontillo G, Quarantelli M, et al. Default mode network modifications in Fabry disease: A resting-state fMRI study with structural correlations. *Hum Brain Mapp*. 2018;39:1755–1764. https://doi.org/10.1002/hbm.23949